

See discussions, stats, and author profiles for this publication at: <https://www.researchgate.net/publication/263958436>

# Flash Cooling Protein Crystals: Estimate of Cryoprotectant Concentration Using Thermal Properties

ARTICLE in CRYSTAL GROWTH & DESIGN · MARCH 2011

Impact Factor: 4.89 · DOI: 10.1021/cg1013939

---

CITATIONS

6

---

READS

60

## 5 AUTHORS, INCLUDING:



**Binal Shah**

University of Illinois at Chicago

10 PUBLICATIONS 74 CITATIONS

SEE PROFILE



**Unmesh Chinte**

Argonne National Laboratory

14 PUBLICATIONS 114 CITATIONS

SEE PROFILE



**Bryant Leif Hanson**

University of Toledo

62 PUBLICATIONS 1,077 CITATIONS

SEE PROFILE



**Constance Schall**

University of Toledo

55 PUBLICATIONS 990 CITATIONS

SEE PROFILE

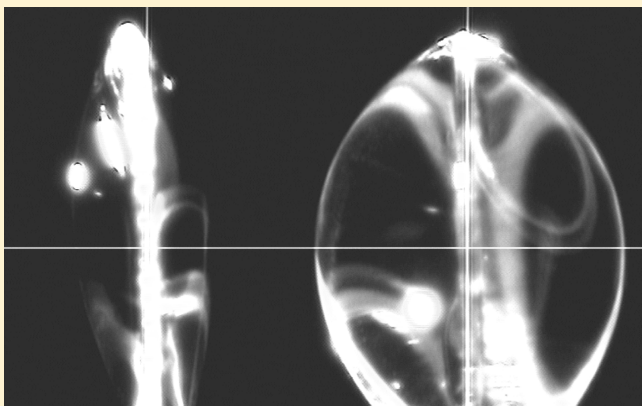
# Flash Cooling Protein Crystals: Estimate of Cryoprotectant Concentration Using Thermal Properties

Published as part of the *Crystal Growth & Design* virtual special issue on the 13th International Conference on the Crystallization of Biological Macromolecules (ICCBM13).

Binal N. Shah,<sup>†,§</sup> Unmesh Chinte,<sup>†,||</sup> Stephen J. Tomanicek,<sup>†,⊥</sup> B. Leif Hanson,<sup>\*,‡</sup> and Constance A. Schall<sup>\*,†</sup>

<sup>†</sup>Department of Chemical and Environmental Engineering, and <sup>‡</sup>Department of Chemistry, University of Toledo, Toledo, Ohio

**ABSTRACT:** X-ray diffraction from protein crystals is routinely measured at cryogenic temperatures, primarily to minimize radiation damage. Protein crystals and the surrounding mother liquor have high water content, which can lead to ice formation when samples are cooled to cryogenic temperatures. Cryoprotectants are added to the aqueous mother liquor solutions to achieve both vitreous water and to retain protein crystal integrity. Finding a minimum cryoprotectant concentration to avoid ice formation is a trial and error procedure, and valuable crystals are often lost in this exercise. To minimize crystal loss, a predictive algorithm for estimation of cryoprotectant concentration requirements for successful flash cooling was developed based on heat transfer analysis and thermal properties of cryoprotectant solutions. These thermal properties such as glass transition temperature, melting temperature, and specific heat capacity were measured and modeled for aqueous glycerol and ethylene glycol solutions, and ternary mixtures of glycerol–salt–water. The minimum amounts of cryoprotectant required for successful flash cooling in samples of varying size were evaluated by X-ray diffraction, and a target cooling time for sample vitrification was identified. A predictive heat transfer analysis and property algorithm for cryoprotectant requirements was verified for neutron diffraction sized crystals of D-xylose isomerase and *Aeropyrum pernix* flap endonuclease 1.



## INTRODUCTION

The 3-dimensional structure of macromolecules is obtained largely from X-ray diffraction data measured on crystals at cryogenic temperatures.<sup>1–4</sup> Exposure of protein crystals to ionizing X-rays results in the formation of photoelectrons and free radicals. These in turn react with the protein, breaking disulfide and other bonds, disordering the lattice and reducing the crystal lifetime in the X-ray beam.<sup>5</sup> At cryogenic temperatures, the diffusion of these radicals is dramatically reduced, thus increasing the crystal lifetime.

Protein crystals contain 10 to 100 Å channels, filled with crystallizing or stabilizing solution. These solutions are mixtures of salts, precipitants, and buffer in an aqueous solution. On cooling to cryogenic temperatures, water within and around the crystal can form ice, giving rise to additional X-ray scattering from ice crystals and potentially disrupting the protein crystal lattice. Formation of crystalline ice can be avoided by rapidly cooling the protein crystal to form a vitreous (glassy) aqueous phase below the glass transition temperature. Pure water and many crystallization solutions require very high cooling rates to achieve this vitreous phase that generally are unavailable with common cryogens. The vitrification of aqueous solutions in protein

crystals can be achieved by mixing cryoprotectants with the crystal stabilizing solution.<sup>1–3,6</sup> Cryoprotectant addition decreases the melting point and the homogeneous nucleation temperature of water, decreasing the temperature window of ice formation.<sup>7,8</sup> Commercial cryostat cooling rates are then rapid enough to form vitreous solutions. However, cryoprotectant selection and concentration is often a trial and error procedure, leading to losses of valuable protein crystals in the process. This article describes a procedure to estimate minimal cryoprotectant concentration for protein crystals to avoid loss of valuable protein crystals during cryo-cooling.

Pure water has a reported glass transition temperature ( $T_g$ ) between 130 and 140 K.<sup>9–17</sup> The homogeneous nucleation temperature of water is reported as 235 K;<sup>18</sup> the melting temperature is 273 K. The temperature window between the homogeneous nucleation and glass transition, the ice nucleation window, must be transited during flash cooling. This transit must be rapid enough to avoid an ice nucleation event. Effective

**Received:** October 18, 2010

**Revised:** February 23, 2011

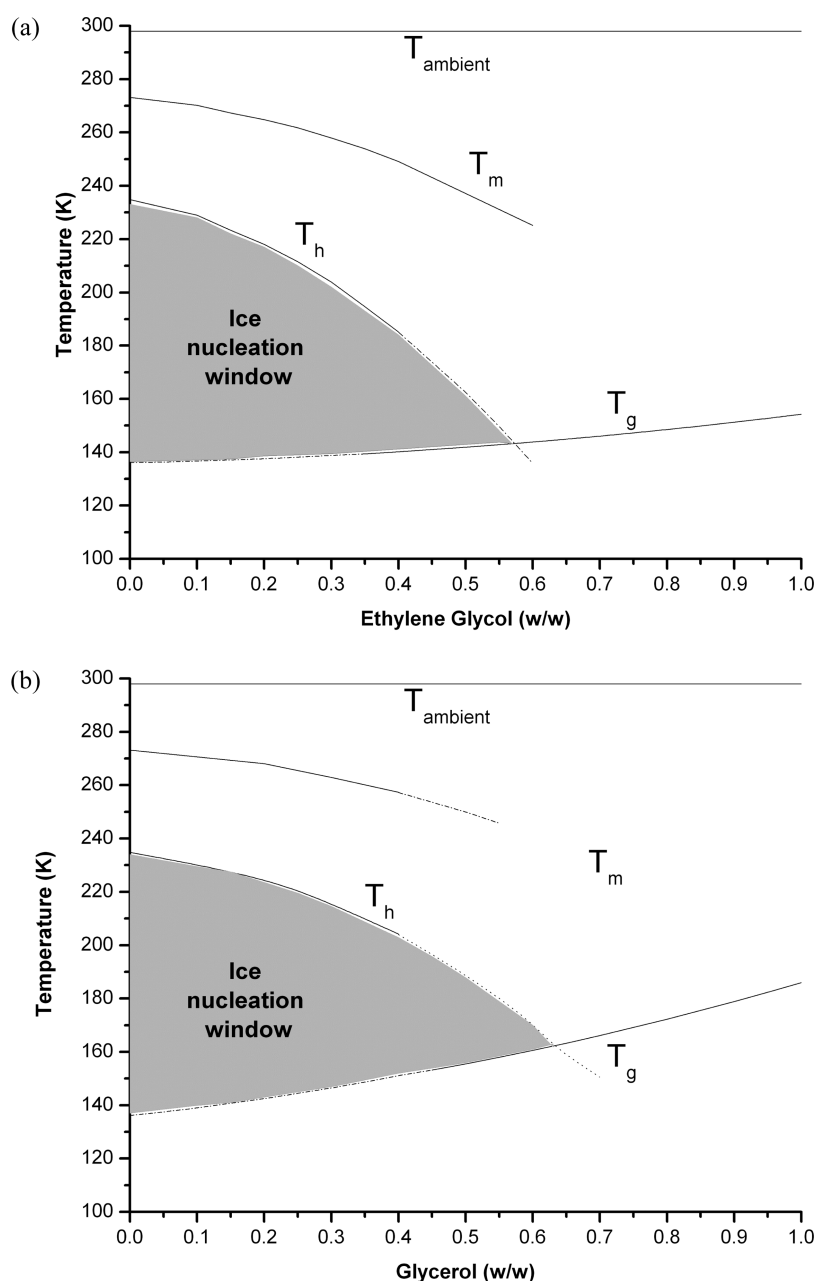


**Figure 1.** Phase diagram for (a) ethylene glycol and water (b) glycerol and water solutions. Data for homogeneous ice nucleation temperature ( $T_h$ ), melting temperature ( $T_m$ ), and for glass transition temperature ( $T_g$ ) are taken from Rasmussen and MacKenzie (refs 18 and 17, respectively).  $T_g$  and  $T_h$  data in the unmeasured range is plotted by extrapolating the data.

cryoprotectants have high glass transition temperatures ( $T_g$ ) and when mixed with water raise the  $T_g$  and lower the homogeneous nucleation temperature ( $T_h$ ) of the resultant solution, reducing the probability of ice nucleation. For example, glycerol has a  $T_g$  of 186–190 K; and ethylene glycol has a  $T_g$  of 155 K. The change in  $T_g$  and  $T_h$  is evident in the experimentally measured properties of aqueous solutions of glycerol and ethylene glycol solutions (Figure 1). Addition of cryoprotectant also can increase solution viscosity, subsequently reducing the ice nucleation rate.<sup>19</sup>

Various parameters that affect the flash cooling step include temperature of cryogen, thermal properties of cryogen, plunging or cooling velocity (including flow rate of cryostream), crystal shape and size, crystal channel size, solvent content within the

channels, type of protein, solvent surrounding the crystal, loop properties, and humidity in the environment. Kriminski et al.<sup>20</sup> examined parameters affecting crystal heating through simulations of crystal cooling and arranged the factors affecting flash cooling from most to least important as follows: (1) crystal solvent content and solvent composition, (2) crystal size and shape, (3) amount of residual liquid around the crystal, (4) cooling method (liquid plunge versus gas stream), (5) choice of gas/liquid, and (6) relative speed between cooling fluid and the crystal. In our earlier paper,<sup>21</sup> we examined the effect of sample size and solution composition on vitrification by flash-cooling in cold nitrogen gas. We found that glass transition temperatures of a selected set of screening solutions mixed with cryoprotectants

lay within a narrow range of values, pointing to a critical or maximum vitrification time interval for successful flash cooling.

Our goal is to develop a protocol to estimate the minimum cryoprotectant requirements to avoid ice formation based on thermal properties and heat transfer analysis. Our specific target is to flash-cool large crystals suitable for neutron diffraction studies, to be able to compare solvent structure in room and low temperature diffraction studies, and preserve crystals at the peak of crystallinity. Two proteins, D-xylose isomerase (XI) from *S. rubiginosus* and flap endonuclease 1 (FEN-1) from *A. pernix* were chosen for study and application of cryoprotection protocols. Specifically, the glass transition temperature and heat capacity were measured for a number of aqueous glycerol and ethylene glycol solutions, the cryoprotectants for XI and FEN-1, respectively. Samples of solutions with dimensions similar to that of large crystals were flash cooled to determine cryoprotectant requirement. By combining the parameters of these solutions with property and heat transfer models, the time needed to vitrify target solutions with volumes similar to those seen for neutron diffraction sized crystals were calculated. An algorithm for estimating cryoprotectant conditions using a target cooling time for sample vitrification was then applied to and demonstrated for XI and FEN-1 crystals.

## ■ EXPERIMENTAL SECTION

**Sample Preparation and Flash Cooling.** Binary aqueous solutions of glycerol (Fisher Scientific, G33-500) and ethylene glycol (Fisher Scientific, E178-4) were made in 2.5% (v/v) increments after removing any residual moisture in glycerol and ethylene glycol using molecular sieves. Ammonium sulfate (Fisher Scientific, A702-3) and sodium chloride (Fisher Scientific, S271-3) solutions were made by weighing the salts into water or aqueous mixtures of cryoprotectants.

The solutions were flash cooled in a flowing nitrogen stream from an Oxford 700 Cryostream operated at a set point of 100 K. The cryostat (aligned with a slight vertical offset) delivers a  $\sim 7$  mm (6.85 mm) diameter cold stream (cryostream) with a flow rate of 5 L per minute at room temperature. The coldest part of the cryostream is located within  $\sim 1$  mm radial distance from the center of the cryostream.<sup>22,23</sup> In practice, the temperature at the crystal position is slightly higher (by  $\sim 5$  K) than the set temperature of the cryostat.<sup>22,23</sup> The distance of the loop from the cryostat nozzle tip was set at 5 mm. As loop size changed, the loop was realigned to the center of the cold stream and 5 mm from the nozzle tip. The plane of the loop was oriented parallel to the cryostream flow direction. Cryoloops were made with 20  $\mu$ m nylon fiber and were purchased from Hampton Research (HR4-941). Loop and sample dimensions were measured by optical microscopy.

Two sets of samples were used in flash cooling experiments. One set included XI crystals and FEN-1 crystals. The second set of samples included cryo-solutions, in the form of bulges on the cryoloop. Drops of solutions were pipetted onto the loop with complete contact made between drop and loop. The sample was then transferred to a goniometer head mounted on a Rigaku FR-E X-ray source with a Saturn 92 CCD detector where the cold nitrogen stream from the cryostat was deflected using a wide ruler as a shutter. The minimum cryoprotectant concentration needed for vitrification was determined within 2.5% (v/v) for samples of cryosolutions of variable size and composition. The minimum cryoprotectant concentration needed for vitrification was determined within 5.0% (v/v) for XI crystal samples of variable size. Cryoprotection selection protocols were tested against FEN-1 crystals.

X-ray diffraction images were collected in three orientations of  $\omega$  scans ( $-50^\circ$ ,  $-5^\circ$ , and  $40^\circ$ ) with  $\phi$  and  $\chi$  angles set at  $0^\circ$ . An exposure time of 5 s was used for loops greater than 0.2 mm. For 0.2 mm an exposure time of 20 s was used. The sample to detector distance was held at 45 mm for all samples. The presence or absence of ice rings in all the three orientations were noted as the concentration of cryoprotectant

changed. A video microscope was used to observe the samples and acquire images of the samples before and after cooling.

**Crystallization and Preparation of Protein Crystals.** D-Xylose isomerase (Hampton Research HR7-100), received as a crystal suspension, was dissolved then dialyzed against 100 mM Tris-HCl, pH 8.0, and 10 mM ethylenediaminetetraacetic acid (EDTA) to remove metal cations. The protein solution was then exchanged with 100 mM Tris-HCl, pH 8.0, and 10 mM  $\text{MgCl}_2$  using a Viva Cell pressure filtration unit (10,000 MWCO) and further concentrated in 10,000 MWCO Centriprep tubes (Amicon). The protein stock, ammonium sulfate, and the buffer solutions were mixed to bring the final concentrations to 10% (w/v) ammonium sulfate, 100 mM Tris-HCl, pH 8.0, and 10 mM  $\text{MgCl}_2$ , and 48 mg/mL protein (for crystallization at  $10^\circ\text{C}$ ) and 52 mg/mL (for crystallization at  $4^\circ\text{C}$ ). Hanging drops of 30  $\mu$ L were suspended on a glass coverslip over a 500  $\mu$ L well solution with ammonium sulfate and buffer concentration matching that of the drop.

Crystals of XI prepared for flash cooling were transferred to a solution of 20% (w/v) ammonium sulfate in 100 mM Tris-HCl, pH 8.0, and 10 mM  $\text{MgCl}_2$ . No crystal dissolution or cracking was observed by optical microscopy under these conditions of mother-liquor. The crystals were then transferred to solutions of increasing glycerol concentration in 5% (v/v) increments maintaining the same overall salt and buffer concentrations as the starting solution (20% ammonium sulfate above). The crystals were immersed in each solution for 60, 120, and 180 s for 0.1,  $< 0.4$ , and 0.8 mm (shortest dimension) crystals, respectively. This immersion time was estimated on the basis of the diffusion coefficient of glycerol and the shortest crystal dimension.<sup>23</sup>

Flap Endonuclease-1 (FEN-1) DNA-repair enzyme from the cre-narchaeal organism *Aeropyrum pernix* was expressed in *E. coli* and purified as previously described.<sup>24</sup> After the FEN-1 protein was purified in hydrogenated buffer solutions, the labile hydrogen atoms were exchanged to deuterium against 50 mM Tris-d11-DCl, pD 7.0, 100 mM  $\text{ND}_4\text{Cl}$ , and 50 mM  $\text{MgCl}_2$  in 99.9%  $\text{D}_2\text{O}$  using a 10,000 MWCO Amicon Ultra-4 (Millipore, USA) concentrator. Prior to concentration for crystallization, the thermostable protein was incubated in deuterated buffer at high temperature;  $75^\circ\text{C}$  for 30 min followed by slow-cooling in  $5^\circ\text{C}$  increments with a 30 min hold until the samples reached  $25^\circ\text{C}$ . Crystals were grown using sitting drop vapor diffusion at  $21^\circ\text{C}$  with shallow gradients of 1–4% PEG 8000 (dissolved in  $\text{D}_2\text{O}$ ), 100 mM deuterated Tris-d11-DCl, pD 7.0, and 25% deuterated ethylene glycol with  $\sim 10$ –15 mg/mL of protein using various protein/reservoir solution volumes. Once crystals were harvested and looped, all cryogenic soaks were completed on ice for  $\sim 3$  min using 300  $\mu$ L of a reservoir solution composed of 100 mM Tris-d11-DCl, pD 7.0, 100 mM  $\text{ND}_4\text{Cl}$ , 50 mM  $\text{MgCl}_2$ , 1% (w/v) PEG 8000, and 30% (w/v) ethylene glycol-d6 made in 99.9%  $\text{D}_2\text{O}$ .

**Heat Capacity and  $T_g$  measurements.** Specific heat capacity,  $C_p$ , measurements were made for aqueous glycerol and ethylene glycol solutions using a differential scanning calorimeter (DSC). Some measurements were also made on ternary systems of glycerol–sodium chloride–water and glycerol–ammonium sulfate–water. A stepscan (isothermal hold–short scan–isothermal hold) or a linear fixed scan method on a Perkin-Elmer Diamond DSC was used to measure the  $C_p$ . Details about calibration and measurements for heat capacity are reported in the Supporting Information.  $T_g$  was measured by DSC as detailed in an earlier paper.<sup>25</sup>

## ■ HEAT TRANSFER AND PROPERTY MODEL DEVELOPMENT

**Heat Transfer Model.** The goal of flash cooling in a cryogenic gas stream is to reach a temperature below the glass transition temperature of the sample in a time short enough to avoid the nucleation of ice. In the absence of surfaces or particles that can serve as ice nucleation sites, ice can nucleate at the homogeneous



ice nucleation temperature,  $T_h$  (methods for estimating  $T_h$  are discussed later). Protein crystallization solutions are filtered or centrifuged to remove particles. This combined with small sample sizes encountered in flash cooling reduce the probability of heterogeneous nucleation. A priori methods for the prediction of heterogeneous nucleation temperatures are not readily available. In the absence of heterogeneous nucleation sites, the temperature region for ice nucleation is between the homogeneous ice nucleation ( $T_h$ ) and the glass transition ( $T_g$ ) temperatures. Addition of cryoprotectant decreases this ice nucleation window between  $T_h$  and  $T_g$ . For a fixed sample size,  $T_g$ 's of Hampton Screen I solutions mixed with minimum glycerol requirements to avoid ice formation were found to be relatively invariant in our prior studies.<sup>21</sup> This points to a critical time that the sample can spend between  $T_g$  and  $T_h$  for successful flash cooling, and will be referred to as a maximum flash cooling time or critical vitrification time,  $t_{vitr}$ :

$$t_{vitr} = t_g - t_h \quad (1)$$

where  $t_h$  is the time to cool a sample from ambient temperature to its homogeneous nucleation temperature ( $T_h$ ), and  $t_g$  is the time to cool a sample from ambient to its glass transition temperature ( $T_g$ ) for a vitrified sample.

During flash cooling, heat is transferred from the core of the sample, to the surface of the sample by conduction and from the surface to the cold gas by convection. The heat transfer analysis can be simplified using a lumped system analysis for low Biot numbers ( $Bi = h\delta/k_s$  is less than 0.1).  $\delta$  can be estimated as the sample thickness,  $k_s$  is the sample thermal conductivity, and  $h$  is the convective heat transfer coefficient. At low values of the Biot number, it can be assumed that the sample cools with no temperature gradients within the sample (conduction is rapid compared to convection). This approach is similar to that used by Kuzay et al.,<sup>26</sup> Krimsinski et al.,<sup>20</sup> and Chinte et al.<sup>21</sup> The time,  $t_{hg}$  required to cool a sample from  $T_h$  to  $T_g$  can be obtained using eq 2.

$$t_{hg} = \frac{\rho_s \langle C_{ps} \rangle V_s}{hA_s} \ln \left( \frac{T_h - T_{N2}}{T_g - T_{N2}} \right) \quad (2)$$

$\rho_s$  is the density of the sample,  $\langle C_{ps} \rangle$  is the temperature average heat capacity of the sample between  $T_g$  and  $T_h$ , and  $V_s$  and  $A_s$  are the volume and surface area of the sample, respectively. The heat transfer coefficient,  $h$  is dependent on the sample geometry and the transport and thermal properties of the cryogen,  $T_{N2}$  is the cryogen temperature (often nitrogen). When  $t_{hg} \leq t_{vitr}$ , the sample is expected to be vitrified.

Properties, such as thermal conductivity, density and heat capacity of the sample, and the transition temperatures ( $T_h$  and  $T_g$ ) are all related to composition and temperature. If the critical vitrification time ( $t_{vitr}$ ) is known, the minimum concentration of cryoprotectant required for successful flash cooling can be estimated. We will now outline the measurement or estimation of parameters required for the calculation of the critical vitrification time.

**Heat Transfer Coefficient ( $h$ ).** The convective heat transfer coefficient,  $h$ , is dependent on sample geometry and the thermal properties of the fluid. A large protein crystal with surrounding solution held in a loop can be represented using ellipsoidal or spherical geometry. These geometries may require finite element analysis for the estimation of  $h$  due to boundary layer separation, which is beyond the scope of this article. Mhasiekar<sup>27–29</sup> studied the thermal modeling of X-ray heating of a biocrystal using a

numerical computational fluid dynamics technique. He calculated the local and average convective heat transfer coefficient for steady flow around crystals of varying size, at constant velocity, subjected to X-ray beam heating. He assumed the crystal in a loop to be spherical in shape. The average Nusselt numbers (first term in eq 3) obtained in his simulations are correlated with Reynolds and Prandtl numbers in a form similar to that used for spheres. The following correlation regressed using least-squares analysis of his calculated  $h$  for constant velocity is used for our estimation of  $h$ .

$$\frac{hD_{eq}}{k_f} = 2 + 0.0137 \left( \frac{D_{eq}u_{\infty}\rho_f}{\mu_f} \right)^{1.333} \left( \frac{C_p\mu_f}{k_f} \right)^{1/3} \quad (3)$$

$D_{eq}$  is the equivalent diameter of a sphere with the same surface to volume ratio as the sample. The subscript  $f$  refers to properties of the cryogenic fluid stream. The surface to volume ratio of the sample can be easily calculated on the basis of the crystal geometry.  $\mu$  is viscosity,  $k$  is thermal conductivity, and  $u_{\infty}$  is the cryostream velocity beyond the boundary layer. The thermal properties of the cryostream (at 105 K) are taken from Weisend.<sup>30</sup>

**Properties of the Sample.** Because of the lack of the thermal properties of protein crystals and the surrounding solutions, thermal properties of the mother liquor with cryoprotectant are used for crystals and solutions. This should provide a conservative estimate of properties, in particular for  $T_g$  and  $T_h$ , since any cryoprotection afforded by protein or small crystal channels is neglected.<sup>31,32</sup>

Room temperature density values were obtained experimentally by calculating the ratio of the solution weight to a known volume of mother-liquor–cryoprotectant mixture. Density can also be crudely estimated assuming no volume change with mixing at known mass fractions ( $M_i$ ) and densities ( $\rho_i$ ) of solution components.

$$\rho_s = \frac{\sum_{i=1}^n M_i}{\sum_{i=1}^n \frac{M_i}{\rho_i}} \quad (4)$$

These room temperature densities were used in eq 2 with the assumption that these values do not exhibit large variation with temperature. Recent studies by Alcorn and Juers<sup>33</sup> with aqueous mixtures of glycerol and ethylene glycol indicate ~2–13% contraction for the cryoprotectant solutions during flash cooling.

**Homogenous Nucleation Temperature.** Addition of solutes to water often increases viscosity and alters other properties resulting in the depression of melting temperature and ice nucleation temperature.<sup>7,8,19,34,35</sup> Franks<sup>36</sup> and Rasmussen<sup>37</sup> used classical nucleation theory to derive a linear relationship between the depression in ice nucleation temperature of water with a depression in melting temperature of ice by the addition of solute (Figure 3) represented by the following equation.

$$T_{h0} - T_h = A(T_{m0} - T_m) \quad (5)$$

$T_{h0}$  is the homogeneous nucleation temperature of pure water (235 K),  $T_h$  is the homogeneous nucleation temperature in a mixture (the unknown).  $T_{m0}$  is the melting temperature of pure ice (273.15 K), and  $T_m$  is the melting temperature of the mixture, which can be readily measured using DSC or a melting point apparatus. The proportionality constant,  $A$  is solute dependent. Rasmussen and MacKenzie<sup>18</sup> have measured the homogeneous nucleation ( $T_h$ ) and melting temperature ( $T_m$ ) of aqueous solutions of glycerol, ethylene glycol, sodium chloride, glucose, urea, polyethylene glycol 9000, and

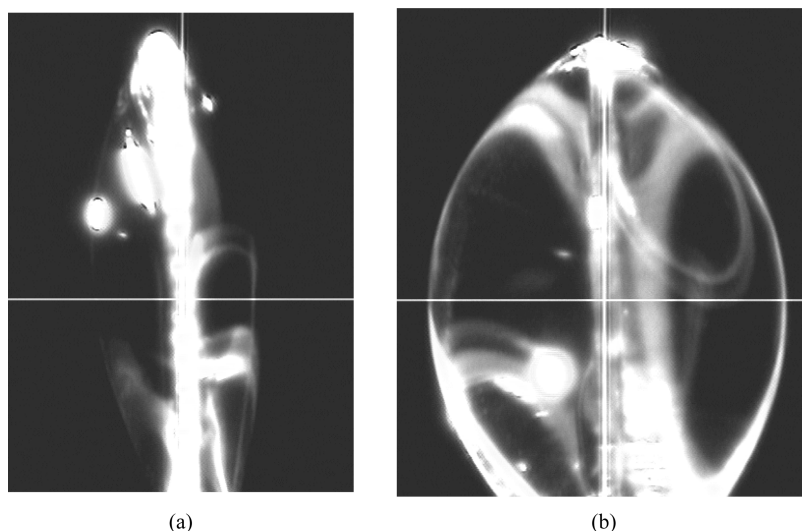


**Figure 2.** Examples of vitrified samples of various thicknesses in the  $0.89 \times 0.47$  mm loop. The figure shows (a) 0.25 mm thick and (b) 0.55 mm thick samples.

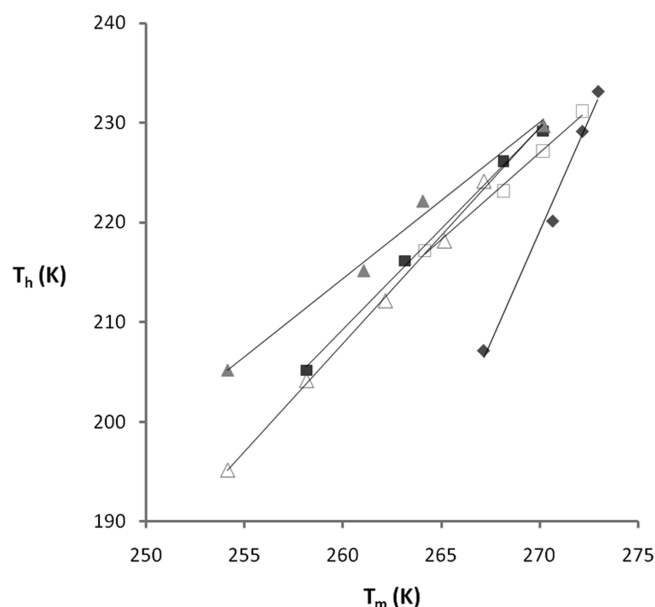


**Figure 3.** Homogenous nucleation temperature ( $T_h$ ) and melting temperature ( $T_m$ ) for varying concentrations of different solutes in water. Glycerol, solid square; Ethylene glycol, open triangle; NaCl, solid triangle; Glucose, open square; PEG, solid diamond. Adapted from Rasmussen and MacKenzie (ref 18).

polyvinyl pyrrolidone. Equation 5 holds well with the constant  $A$  varying from solute to solute. Other researchers have also measured the homogeneous ice nucleation temperature for various alcohols and saccharides<sup>38</sup> and salts such as magnesium chloride, calcium nitrate and lithium chloride in water,<sup>39</sup> and polyethylene glycol.<sup>40</sup> The linear correlation for some of the solutes is shown in Figure 3 which is adapted from Rasmussen and MacKenzie.<sup>18</sup> For most of the solutes,  $A$  is between 1.5 and 2.0, except for PEG for which the value increases to 5.0 up to a molecular weight of 1000.<sup>40</sup> In these studies,  $T_h$  for binary solutions is used from Rasmussen and MacKenzie, whereas for ternary or multicomponent solutions,  $T_h$  is calculated using eq 5 using measured  $T_m$  of the mixture with an

value of 1.946 and 2.087 for glycerol–water and ethylene–glycol binary solutions, respectively.

**Glass Transition Temperature ( $T_g$ ).** Solutions used in flash cooling are multicomponent mixtures with salts, precipitants, and buffers along with cryoprotectants. The models that relate glass transition temperature to composition for aqueous solutions<sup>10,39,41–52</sup> and polymeric materials<sup>53,54</sup> lack the predictive capability for multicomponent systems largely used in flash cooling protein solutions. In an earlier paper,<sup>25</sup> we measured the glass transition temperature of a selected set of multicomponent solutions. The  $T_g$  of multicomponent solutions was found to be well predicted by a combination of the Fox equation<sup>53,54</sup> and Miller's equation.<sup>52</sup> This Miller/Fox eq 6 yielded  $T_g$  within  $\pm 4$  K of the experimental values.

$$\frac{1}{T_g} = \sum_i^n \frac{m_i}{m_i T_{gi}} \frac{\rho_i}{\rho_s} \quad (6)$$

$\rho_s$  is the density of the solution mixture, and  $\rho_i$  is the density of pure component  $i$ .  $T_{gi}$  is the glass transition temperature of pure component  $i$ . Salts and buffers do not exhibit a glass transition, and their  $T_g$  can be empirically estimated from the more experimentally accessible melting temperature and by assuming  $T_g/T_m$  is equal to  $2/3$ .<sup>10,55,56</sup>  $T_g$  values used in these studies are either experimentally measured values or those calculated from eq 6.

**Temperature Dependent Heat Capacity.** To the best of our knowledge, specific heat capacity for aqueous cryoprotectant solutions or for multicomponent solutions is not available in literature in the cryogenic and supercooled temperature ranges. For aqueous glycerol and ethylene glycol solutions,  $C_p$  was measured using DSC, primarily with a stepscan method (Supporting Information). A temperature average heat capacity between  $T_h$  and  $T_g$  is used for our analysis as described in Supporting Information.

## RESULTS AND DISCUSSION

The critical vitrification time was determined by calculating time spent by samples between  $T_h$  and  $T_g$  (eq 2, by equating  $t_{hg} = t_{vitr}$ ), for aqueous solution samples successfully cryoprotected with glycerol or ethylene glycol using minimal cryoprotectant

**Table 1. Critical Vitrification Times Estimated for Aqueous Solutions of Glycerol and Ethylene Glycol in Varying Thicknesses (Bulges, Figure 2) for Two Different Loop Sizes ( $1.49 \times 0.71$  mm and  $0.89 \times 0.47$  mm) Using the Heat Transfer Coefficient Correlation Developed for Constant Cryogen Velocity Using eq 3<sup>27,29a</sup>**

$2a \times 2b \times 2c$ (mm <sup>3</sup> )	$x$ % (v/v)	$T_h$ (K) <sup>b</sup>	$T_g$ (K)	$\rho_s$ (kg/m <sup>3</sup> )	$\langle C_{ps} \rangle$ (J kg <sup>-1</sup> K <sup>-1</sup> )	$k_s$ (W m <sup>-1</sup> K <sup>-1</sup> )	$h$ (W m <sup>-2</sup> K <sup>-1</sup> )	$t_{vitr}$ (s)
Glycerol–Water Solutions								
$1.49 \times 0.71 \times 0.49$	35	204.3	152.1	1092	2086	0.4527	307	0.64
$0.89 \times 0.47 \times 0.33$	32.5	207.5	149.1	1086	1964	0.4615	287	0.48
Ethylene Glycol Solutions								
$1.49 \times 0.71 \times 0.63$	40	180.9	142.3	1052	2006	0.4445	316	0.63
$1.49 \times 0.71 \times 0.74$	40	180.9	142.3	1052	2006	0.4445	321	0.66
$0.89 \times 0.47 \times 0.18$	30	200.2	141.9	1040	2164	0.4810	280	0.39
Glycerol–8% (w/v) Sodium Chloride–Water								
$1.49 \times 0.71 \times 0.75$	30	186.0	160.3	1114	1929	0.4961	322	0.36
$0.89 \times 0.47 \times 0.30$	27.5 <sup>c</sup>	194.0	149.9	1112	1576	0.4850	324	0.27
Glycerol–20% (w/v) Ammonium Sulfate–Water								
$1.49 \times 0.71 \times 0.45$	25	188.3	157.9	1071	1827	0.4841	306	0.33
$0.89 \times 0.47 \times 0.25$	25	188.3	157.9	1071	1827	0.4841	282	0.20
$0.89 \times 0.47 \times 0.48$	25	188.3	157.9	1071	1827	0.4841	295	0.28
$0.89 \times 0.47 \times 0.55$	25	188.3	157.9	1071	1827	0.4841	297	0.29

<sup>a</sup> The cryoprotectant concentration was varied in 2.5% increments until no ice diffraction was observed in the X-ray data. <sup>b</sup>  $T_h$  (K) for binary solutions is taken from Rasmussen and Mackenzie<sup>18</sup> for salt solutions and are calculated from the equation  $T_h = T_{h0} + A(T_{m0} - T_m)$ , where  $A$  is 1.946 for glycerol,  $T_{m0}$  and  $T_{h0}$  are the melting temperature (273 K) and homogeneous nucleation temperature ( $\sim 234.8$  K), respectively, for water.  $T_m$  is the melting temperature, measured at the peak of melting from a DSC curve (data not shown).  $T_g$  is measured as reported in Shah and Schall.<sup>25</sup> <sup>c</sup> A faint ring was observed in the diffraction data in one orientation.

(within  $\pm 2.5\%$ ). Samples include binary mixtures and ternary mixtures of glycerol–salt–water for bulge (ellipsoidal) shaped samples (Figure 2). The results so obtained are summarized in Table 1. The vitrification times vary from 0.20 to 0.66 s with an average of  $0.41 \pm 0.17$  s for both binary and ternary mixtures. Some of this variability may be due to variation in ice nucleation rates. A number of factors affect nucleation rate, including solution viscosity.<sup>19</sup> Nucleation rates decrease with increasing viscosity. Viscosity increases with increasing glycerol and ethylene glycol concentrations, which would lead to increasing  $t_{vitr}$ . This trend is observed in Table 1.

Our calculated critical vitrification times are on the order of experimentally measured temperature transit times of cryoprotectants in thermocouple loops by Teng and Moffat.<sup>57</sup> In those studies, sample temperature as a function of time was measured for solutions of varying thicknesses (125 and 450  $\mu$ m) held in an  $\sim 1.5$  mm loop made by a thermocouple and flash cooled with a nitrogen cryostat. Cryoprotectant solutions included 20% (v/v) glycerol, 20% (w/w) sucrose, and 30% (v/v) PEG (molecular weight is not mentioned) in 3.4 M ammonium acetate, pH 4.7, and 3.2 M phosphate buffer, pH 7.0. The temperature region of 250 to 150 K is the approximate ice nucleation range. Samples transited the region between 250 to 150 K in approximately  $\sim 0.4$  s ( $\pm 15\%$ ) for thin samples and  $\sim 0.8$  s ( $\pm 10\%$ ) for thick samples.

The minimum amount of glycerol required to successfully flash cool XI crystals of varying size was determined within  $\pm 5\%$  (v/v).<sup>23</sup> The mother liquor solution consists of 20% (w/v) ammonium sulfate in 100 mM Tris-HCl, pH 8.0, and 10 mM MgCl<sub>2</sub>. Aqueous mixtures of glycerol and water were prepared and the buffer and salt concentration was kept at the same concentration as the mother liquor. The critical vitrification time was calculated using room temperature densities and the temperature average heat capacities of the cryoprotected solutions

assuming a lumped system (eq 2, by equating  $t_{hg} = t_{vitr}$ ). Biot numbers were less than 0.08 in all cases.  $T_h$  is estimated in a similar manner, as outlined in the prior section for ternary mixtures. The heat transfer coefficient correlations were obtained from eq 3. An average value of  $t_{vitr}$  of  $\sim 0.29 \pm 0.09$  s was found for four crystals. Combined with the data for bulges of solutions, an overall average of  $\sim 0.38$  s was found for  $t_{vitr}$  and used as a target time of transit through the ice nucleation window,  $t_{hg}$ . In the section below, we provide an example of calculations performed to estimate the minimum cryoprotectant concentration for a large protein crystal based on a target  $t_{hg}$ .

**Calculation Algorithm for Determining Cryoprotectant Concentration.** We use a target cooling time ( $t_{hg}$ ) of 0.38 s for a XI crystal of approximate dimensions of 0.8 mm  $\times$  0.8 mm  $\times$  0.35 mm. The stable mother liquor for this crystal is 20% (w/v) ammonium sulfate, in 100 mM Tris-HCl, pH 8.0, and 10 mM MgCl<sub>2</sub>. Aqueous glycerol is selected as the cryoprotectant. The concentration of all salts is maintained at that of the stable mother liquor on a weight per volume basis in the water/glycerol mixture. The glycerol concentration is varied until the resultant cooling time between  $T_h$  and  $T_g$  is equal to or under 0.38 s.

Equation 2 gives a relationship between  $t_{hg}$  (time between  $T_h$  and  $T_g$ ) and crystal and transport properties. For a successfully flash cooled sample with minimum cryoprotectant,  $t_{hg}$  is less than or equal to the critical vitrification time ( $t_{vitr}$ ). Mother liquor properties of average  $\rho_s$ ,  $C_{ps}$ ,  $T_h$ , and  $T_g$  are used as an estimate of the sample (crystal plus mother liquor).

$$t_{vitr} = \frac{\rho_s \langle C_{ps} \rangle V_s}{h A_s} \ln \left( \frac{T_h - T_{N2}}{T_g - T_{N2}} \right)$$

The surface volume  $D_{eq}$  is the equivalent diameter of a sphere with the same surface to volume ratio as the sample calculated as



shown below:

$$\begin{aligned} & \left( \frac{V_s}{A_s} \right)_{\text{crystal}} \\ &= \frac{0.8 \times 0.8 \times 0.35}{(2. \times 0.8 \times 0.8) + (2 \times 0.8 \times 0.35) + (2 \times 0.35 \times 0.8)} \\ &= 0.09377 \text{ mm} \\ & \left( \frac{V_s}{A_s} \right)_{\text{crystal}} = \left( \frac{V_s}{A_s} \right)_{\text{sphere}} = \frac{D_{eq}}{6} \quad (7) \\ & D_{eq} = 0.56 \text{ mm} \end{aligned}$$

The heat transfer coefficient is estimated using eq 3. The crystal is to be cooled in a cold nitrogen stream set at 100 K (105 K at the crystal position) using an Oxford 700 cryostat. The flow of  $N_2$  is set at room temperature at a flow rate of 5 L/min. The density of nitrogen at room temperature is  $1.1308 \text{ kg/m}^3$ . This gives a mass flow rate of  $9.423 \times 10^{-5} \text{ kg/s}$ . The cross-sectional area of the cold stream is  $\sim 6.85 \text{ mm}$ . The measured temperature at the crystal position ( $\sim 5 \text{ mm}$ ) from the nozzle tip was 105 K. The density ( $\rho_{fl}$ ), heat capacity ( $C_{pfl}$ ), viscosity ( $\mu_{fl}$ ), and thermal conductivity ( $k_{fl}$ ) of cold  $N_2$  at 105 K are  $3.2642 \text{ kg/m}^3$ ,  $1066.5 \text{ J kg}^{-1} \text{ K}^{-1}$ ,  $7.29 \times 10^{-6} \text{ Pa s}$ , and  $0.010378 \text{ Wm}^{-1} \text{ K}^{-1}$ .<sup>30</sup> The mass flow rate of  $9.423 \times 10^{-5} \text{ kg/s}$  gives a velocity of  $0.783 \text{ m/s}$  using the density of  $N_2$  at 105 K. Substitution of these values in eq 3 gives a value of  $\sim 296 \text{ W m}^{-2} \text{ K}^{-1}$  for the heat transfer coefficient.

Other properties required to calculate the cooling time ( $t_{hg}$ ) are the sample thermal properties and transition temperatures. These properties are dependent on composition and/or temperature, thus involving iterative steps. Initially, assume a cryoprotectant concentration, calculate the time,  $t_{hg}$ , using the thermal properties, and check this against the target value of 0.38 s for vitrification. In this case, 30% (v/v) glycerol solution with 20% (v/v) ammonium sulfate in 100 mM Tris-HCl, pH 8.0, and 10 mM  $MgCl_2$  was first assumed, and the sample properties required to calculate  $t_{hg}$  are estimated as follows.

**Density of Solution ( $\rho_s$ ).** The density of 30% (v/v) glycerol, 20% (w/v) solution in 100 mM Tris-HCl, pH 8.0, and 10 mM  $MgCl_2$  was measured as  $1172 \text{ kg/m}^3$ . Density can also be estimated using the mass fractions ( $M_i$ ) and densities ( $\rho_i$ ) of components present using eq 4. The weight fractions of glycerol, water, ammonium sulfate, Tris-HCl, and  $MgCl_2$  are 0.3155, 0.5075, 0.1698, 0.006187, and 0.001036, respectively, and the densities are 1256, 997, 1770, 1237, and  $2325 \text{ kg/m}^3$ , respectively. This gives a calculated density of  $1160 \text{ kg/m}^3$ .

$$\begin{aligned} \rho_s &= \frac{0.3155 + 0.5075 + 0.1678 + 0.006187 + 0.001036}{\frac{0.3155}{1256} + \frac{0.5075}{997} + \frac{0.1698}{1770} + \frac{0.006187}{1237} + \frac{0.001036}{2325}} \\ &\approx 1160 \text{ kg/m}^3 \end{aligned}$$

**Nucleation Temperature ( $T_h$ ).** The ice nucleation temperature of the solution is approximated from the depression in melting point due to the addition of glycerol using eq 5. For glycerol, the  $A$  is  $\sim 1.946$  and can be calculated using measured  $T_m$  values.  $T_m$  can be easily measured using a benchtop melting temperature device or from a calibrated DSC. In this case,  $T_m$  (peak value) was measured by DSC for a 30% (v/v) glycerol solution in mother

liquor as 249 K. The nucleation temperature is calculated as follows:

$$T_h = T_{h0} + 1.946(T_m - T_{m0})$$

$$T_h = 234.85 + 1.946(249 - 273.15) = 187.9 \text{ K}$$

**Glass Transition Temperature ( $T_g$ ).** The glass transition temperature can be measured using a DSC or can be calculated using the Miller/Fox equation (eq 6), using the known weight fractions ( $M_i/M_t$ ) and density of individual components ( $\rho_i$ ) and density of the solution ( $\rho_s$ ). For a 30% (v/v) glycerol with 20% (w/w) ammonium sulfate, 100 mM Tris-HCl, pH 8.0, and 10 mM  $MgCl_2$ , the weight fractions of glycerol, water, ammonium sulfate, Tris-HCl, and  $MgCl_2$  are 0.3155, 0.5075, 0.1698, 0.006187, and 0.001036, respectively, and the densities are 1256, 997, 1770, 1237, and  $2325 \text{ kg/m}^3$ , respectively. The glass transition temperatures of glycerol, water, ammonium sulfate, Tris-HCl, and  $MgCl_2$  are 186 K, 138 K, 369 K, 270 K, and 658 K, respectively. ( $T_g$  of salts is approximated from melting temperature using 2/3 rule<sup>25</sup>.) This gives a calculated glass transition temperature ( $T_g$ ) of the mixture as 162.1 K.

$$\begin{aligned} \frac{1}{T_g} &= \frac{0.3155}{186 \left( \frac{1256}{1160} \right)} + \frac{0.5075}{138 \left( \frac{997}{1160} \right)} + \frac{0.1698}{369 \left( \frac{1770}{1160} \right)} \\ &\quad + \frac{0.006187}{270 \left( \frac{1238}{1160} \right)} + \frac{0.001036}{658 \left( \frac{2325}{1160} \right)} \end{aligned}$$

This compares very well with the  $T_g$  of 161.2 K measured by DSC for 30% (v/v) glycerol 20% (w/v) ammonium sulfate solution in 100 mM Tris-HCl, pH 8.0, and 10 mM  $MgCl_2$ .

**Temperature Average Heat Capacity.** The temperature average heat capacity is calculated between  $T_h$  and  $T_g$  using heat capacity data (Supporting Information). For 30% (v/v) glycerol, the mass ratio of glycerol to glycerol–water is 0.3833, which is close to a 32.5% (v/v) glycerol. Variation of heat capacity with temperature is obtained for 32.5% (v/v) glycerol.

$$\langle C_{ps} \rangle = \left( \frac{8.314}{25.755} \right)$$

$$\frac{\int_{162}^{189} [-35.4766 + 0.4404T - 1.44 \times 10^{-3}T^2 + 1.6389 \times 10^{-6}T^3]dT}{189 - 162}$$

This gave a temperature average value of  $1.919 \text{ J g}^{-1} \text{ } ^\circ\text{C}^{-1}$ .

Using the above values, the calculated cooling time using eq 2 for the first guess of 30% (v/v) glycerol and 20% (w/v) ammonium sulfate in 100 mM Tris-HCl buffer, pH 8.0, and 10 mM  $MgCl_2$  is 0.26 s. This is under the target value of 0.38 s. The above-mentioned calculations were repeated for 25% (v/v) glycerol with 20% (w/v) ammonium sulfate in 100 mM Tris-HCl, pH 8.0, and 10 mM  $MgCl_2$ , and  $t_{hg}$  was calculated as 0.34 s, which is close to the target time of 0.38 (Table 2). The experimentally obtained minimum cryoprotectant concentration to avoid ice formation is 25% (v/v) glycerol<sup>23</sup> for a crystal of these dimensions. Thus, this method gives a prediction of cryoprotectant requirement within  $\pm 5\%$  glycerol.

**Cryocooling of a FEN-1 Crystal.** Since the above method was found to be successful for predicting the cryoprotectant concentrations for XI crystals, it was applied to a FEN-1 crystal.



**Table 2. Critical Vitrification Times for Different Sizes of D-Xylose Isomerase Crystals, Flash Cooled Using an Oxford 700 Cryostream<sup>a</sup>**

$2a \times 2b \times 2c$ (mm <sup>3</sup> )	$x$ % (v/v) Gly. <sup>b</sup>	$T_h$ (K) <sup>d</sup>	$T_g$ (K)	$\rho_s$ (kg/m <sup>3</sup> )	$\langle C_{ps} \rangle$ (J kg <sup>-1</sup> K <sup>-1</sup> )	$k_s$ (W m <sup>-1</sup> K <sup>-1</sup> )	$h$ (W m <sup>-2</sup> K <sup>-1</sup> )	$t_{vitr}$ (s)
$0.2 \times 0.2 \times 0.1$	10	216.1	153.2	1132	2297	0.4959	306	0.17
$0.6 \times 0.6 \times 0.3$	20	204.8	157.5	1156	1910	0.5200	287	0.37
$0.8 \times 0.8 \times 0.35$	25	195.1	159.7	1167	1913	0.5013	296	0.34
$2.1 \times 1.7 \times 0.8^c$	30–35	174.5	163.6	1189	1547	0.4615	357	0.24

<sup>a</sup> The mother liquor consists of  $x$  % (v/v) glycerol (Gly) in 20% (w/v) ammonium sulfate in 100 mM Tris-HCl at pH 8.0 and 10 mM MgCl<sub>2</sub>.  $t_{vitr}$  is calculated assuming a sphere of equivalent (V/A) and using a heat transfer coefficient from eq 3. <sup>b</sup> Data taken from Chinte.<sup>23</sup> <sup>c</sup> For the 2 mm crystal,  $T_g$  and  $T_h$  were estimated at 30% glycerol concentration. <sup>d</sup> Thermal conductivity ( $k_s$ ) is estimated from glycerol–water systems. Density is measured using a four-place analytical balance.  $C_{ps}$  of glycerol–water for 10% (v/v) and 35% (v/v) is used. For 20% (v/v) and 25% (v/v),  $C_{ps}$  of a glycerol–20% (w/v) ammonium sulfate–water solution is used.

FEN-1 is a 40.1 kDa protein with a crystal solvent content of ~51.1%. The crystals of FEN-1 used for neutron diffraction studies crystallize in the  $P6_1$  space group with unit cell edges of  $a = b = 92.84$  and  $c = 80.89$ . Within the FEN-1 crystal, solvent channels are ~40 Å in diameter, similar to those found in XI. A FEN-1 crystal ( $1.49 \times 0.5 \times 0.5$  mm<sup>3</sup>) was stable in a deuterated solution of 100 mM Tris-DCl, pH 7.0, 100 mM ND<sub>4</sub>Cl, 50 mM MgCl<sub>2</sub>, 1% (w/v) PEG 8000, and 30% (w/v) ethylene glycol-d<sub>6</sub> made in D<sub>2</sub>O. This stable mother liquor had a glass transition temperature of 166 K (estimated using the method described by Shah and Schall<sup>25</sup>).  $T_h$  and  $\langle C_p \rangle$  are estimated to be 181 K and 2155 J kg<sup>-1</sup> °C<sup>-1</sup> based on ratio of ethylene glycol to ethylene glycol and water. The cooling time using eq 2 and for  $h$  from eq 3 is 0.22 s, which is less than the critical time of 0.38 s. Thus, no additional cryoprotectant is required for flash cooling with gaseous N<sub>2</sub> at 105 K. This was indeed found to be true.

## CONCLUSIONS

A method is developed on the basis of the thermal and transport properties of crystallizing solutions and cryogen to calculate a conservative estimate of cryoprotectant concentration that would avoid ice formation during the flash cooling step in cryocrystallography. This may help in preventing the loss of valuable crystals due to unsuccessful flash cooling trials. If the sample (protein crystal with surrounding solution held in a loop) is cooled between the homogeneous nucleation temperature and glass transition temperature, in a time period less than a critical vitrification time (on the order of 0.38 s in our studies), the formation of ice is avoided. An approximate cryoprotectant concentration can be assumed, and time spent between  $T_h$  and  $T_g$  ( $t_{hg}$ ) can be calculated on the basis of the thermal properties and heat transfer equations developed herein. The procedure is developed on the basis of a heat transfer model and thermal properties related to composition and temperature for aqueous cryoprotectant solutions, ternary mixtures of glycerol–ammonium sulfate–water, and glycerol–salt–water and complex mixtures.

Proteins may provide additional cryoprotection during flash cooling, especially for crystals with small channel sizes and/or very low solvent content. Using estimates of  $T_h$  and  $T_g$  for mother liquor and cryoprotectant solution alone can provide a conservative estimate of cryoprotection required for crystal/mother liquor systems. The heat transfer model could be strengthened if thermal properties of protein crystals of differing solvent content were available.

The deviations in critical vitrification times between sample geometries can be due to the variability in correlations used for the estimation of heat transfer coefficients. For example, the

estimation of heat transfer coefficients for ellipsoidal or spherical samples should include spatial variation of flow and temperature. This requires a complex computational approach. The simplified approach used here can serve as a starting point to estimate cryoprotectant requirements and is not expected to yield quantitative prediction of sample cooling history.

## ASSOCIATED CONTENT

**S Supporting Information.** Materials and methods used for heat capacity measurements and the modeling of the heat capacity with respect to temperature for various solutions used in this article. This material is available free of charge via the Internet at <http://pubs.acs.org>.

## AUTHOR INFORMATION

### Corresponding Author

\*E-mail: [bryant.hanson@utoledo.edu](mailto:bryant.hanson@utoledo.edu) (B.L.H.); [constance.schall@utoledo.edu](mailto:constance.schall@utoledo.edu) (C.A.S.).

### Present Addresses

<sup>§</sup>Rosalind Franklin University of Medicine & Science, North Chicago, IL.

<sup>||</sup>SERCAT, APS, ANL, Argonne, IL.

<sup>⊥</sup>Environmental Sciences Division, ORNL, Oak Ridge, TN

## ACKNOWLEDGMENT

This research was sponsored by the National Aeronautics and Space Administration grant NAG8-1838 and by The National Science Foundation grant 446218.

## REFERENCES

- Garman, E. *Acta Crystallogr.* **1999**, D55, 1641–1653.
- Garman, E. F.; Schneider, T. R. *J. Appl. Crystallogr.* **1997**, 30, 211–237.
- Hope, H. *Acta Crystallogr.* **1988**, B44, 22–26.
- Rodgers, D. W. *Structure* **1994**, 2 (12), 1135–1140.
- Garman, E. F.; *Acta Crystallogr., Sect. D* **2010**, (Pt 4), 339–351.
- Parkin, S.; Hope, H. *J. Appl. Crystallogr.* **1998**, 31, 945–953.
- Koop, T. Z. *Phys. Chem.* **2004**, 218, 1231–1258.
- Koop, T.; Lue, B.; Tsias, A.; Peter, T. *Nature* **2000**, 406, 611.
- McMillan, J. A.; Los, S. C. *Nature* **1965**, 206, 806–807.
- Angell, C. A.; Sare, E. J. *J. Chem. Phys.* **1970**, 52 (3), 1058–1068.
- Johari, G. P. *Philos. Mag.* **1977**, 35 (4), 1077–1090.
- Mishima, O.; Stanley, H. E. *Nature* **1998**, 396, 329–335.

- (13) Hallbrucker, A.; Mayer, E.; Johari, G. P. *J. Phys. Chem.* **1989**, *93*, 4986–4990.
- (14) Hallbrucker, A.; Mayer, E.; Johari, G. P. *Philos. Mag. B* **1989**, *60* (2), 179–187.
- (15) Johari, G. P.; Hallbrucker, A.; Mayer, E. *Nature* **1987**, *330*, 552–553.
- (16) Sugisaki, M.; Hiroshi, S.; Syuzo, S. *Bull. Chem. Soc. Jpn.* **1968**, *41*, 2591–2599.
- (17) Rasmussen, D. H.; MacKenzie, A. P. *J. Phys. Chem.* **1971**, *75* (7), 967–973.
- (18) Rasmussen, D. H.; MacKenzie, A. P. In *Effect of Solute on Ice-Solution Interfacial Free Energy. Calculation from Measured Homogeneous Nucleation Temperatures*; 161st National Meeting of the American Chemical Society, Los Angeles, CA, 1972; Jellinek, H. H. G., Ed.; Plenum Press, New York, 1972; pp 126–145.
- (19) Karlsson, J. O. M.; Cravalho, E. G.; Toner, M. *J. Appl. Phys.* **1994**, *75* (9), 4442–4455.
- (20) Kriminski, S.; Kazmierczak, M.; Thorne, R. E. *Acta Crystallogr., Sect. D* **2003**, *59*, 697–708.
- (21) Chinte, U.; Shah, B.; DeWitt, K.; Kirschbaum, K.; Pinkerton, A. A.; Schall, C. *J. Appl. Crystallogr.* **2005**, *38* (3), 412–419.
- (22) Alkire, R. W.; Duke, N. E. C.; Rotella, F. J. *J. Appl. Crystallogr.* **2008**, *41*, 1122–1133.
- (23) Chinte, U. Optimization of Cryogenic Cooling of Protein Crystals. Ph.D. Thesis, The University of Toledo, Toledo, OH, 2006.
- (24) Collins, B. K.; Tomanicek, S. J.; Lyamicheva, N.; Kaiser, M. W.; Mueser, T. C. *Acta Crystallogr., Sect. D* **2004**, *60*, 1674–1678.
- (25) Shah, B.; Schall, C. *Thermochim. Acta* **2006**, *443* (1), 78–86.
- (26) Kuzay, T.; Kazmierczak, M.; Hsieh, B. J. *Acta Crystallogr., Sect. D* **2001**, *57*, 69–81.
- (27) Mhaisekar, A. Steady Conjugate Heat Transfer Analysis from X-ray Heated Spherical Biocrystal to Laser Heated Sphere in Steady Laminar Flow at Low Reynolds Number. Ph.D. Thesis, University of Cincinnati, Cincinnati, OH, 2004.
- (28) Mhaisekar, A.; Kazmierczak, M.; Banerjee, R. *Numer. Heat Transfer, Part A* **2005**, *47*, 849–874.
- (29) Mhaisekar, A.; Kazmierczak, M. J.; Banerjee, R. *J. Synchrotron Radiat.* **2005**, *12* (3), 318–328.
- (30) Weisend, J. G., II. *Handbook of Cryogenic Engineering*; Taylor & Francis: Philadelphia, PA, 1998.
- (31) Weik, M.; Kryger, G.; Schreurs; Bouma, B.; Gros, P.; Kroon, J. *Acta Crystallogr., Sect. D* **2001**, *57*, 566–573.
- (32) Shah, B. N. Protein Crystals and Crystallizing Solutions: Thermal and Transport Property Measurement and Correlation for Applications in Flash Cooling Protocols. Ph.D. Thesis, University of Toledo, Toledo, OH, 2007.
- (33) Alcorn, T.; Juers, D. H. *Acta Crystallogr., Sect. D* **2010**, *66*, 366–373.
- (34) Zettlemoyer, A. C. *Nucleation*; Marcel Dekker, Inc.: New York, 1969.
- (35) Debenedetti, P. G., *Metastable Liquids Concepts and Principles*; Princeton University Press: Princeton, NJ, 1996.
- (36) Franks, F. *CryoLetters* **1981**, *2*, 27–31.
- (37) Rasmussen, D. *J. Cryst. Growth* **1982**, *56*, 56–66.
- (38) Miyata, K.; Kanno, H. *J. Mol. Liq.* **2005**, *119*, 189–193.
- (39) Angell, C. A.; Sare, E. J.; Donnelly, J.; MacFarlane, D. R. *J. Phys. Chem.* **1981**, *85* (11), 1461–1464.
- (40) Zobrist, B.; Weers, U.; Koop, T. *J. Chem. Phys.* **2003**, *118* (22), 10254–10261.
- (41) Cruickshank, J.; Hubbard, H. V. S. A.; Boden, N.; Ward, I. M. *Polymer* **1995**, *36* (19), 3779–3781.
- (42) Angell, C. A. *Chem. Rev.* **2002**, *102*, 2627–2650.
- (43) Jochem, M.; Krober, C. *Cryobiology* **1987**, *24*, 513–536.
- (44) Zhao, G.; Guo, X.; He, L.; Liu, Z.; Gao, D. *Thermochim. Acta* **2004**, *419*, 131–134.
- (45) Reid, D. S. *CryoLetters* **1985**, *6*, 181–188.
- (46) Jenckel, E.; Heusch, R. *Kolloid-Zeitschrift* **1953**, *130*, 89–105.
- (47) Gordon, J. M.; Rouse, G. B.; Gibbs, J. H.; Rissen, W. M. *J. Chem. Phys.* **1977**, *66* (11), 4971–4976.
- (48) Couchman, P. R. *Macromolecules* **1987**, *20*, 1712–1717.
- (49) Couchman, P. R.; Karasz, F. E. *Macromolecules* **1978**, *11* (1), 117–119.
- (50) Lesikar, A. V. *J. Chem. Phys.* **1978**, *68* (7), 3323–3325.
- (51) Lesikar, A. V. *Phys. Chem. Glasses* **1975**, *16* (4), 83–90.
- (52) Miller, D. P.; de Pablo, J. J.; Corti, H. *Pharm. Res.* **1997**, *14* (5), 578–590.
- (53) Fox, T. G. *Bull. Am. Phys. Soc* **1956**, *2* (1), 123.
- (54) Feldstein, M. M.; Shandryuk, G. A.; Plate, N. A. *Polymer* **2001**, *42*, 971–979.
- (55) Kanno, H. *J. Non-Cryst. Solids* **1981**, *44*, 409–413.
- (56) Lindemann, F. A. *Phys. Chem.* **1910**, *11*, 609–612.
- (57) Teng, T.-Y.; Moffat, K. *J. Appl. Crystallogr.* **1998**, *31*, 252–257.